β-Phosphorus Hyperfine Coupling Constant in Nitroxides: 6. Solvent Effect in Non-Cyclic Nitroxides

Journal:	*Organic & Biomolecular Chemistry*
Manuscript ID	OB-ART-02-2016-000359.R1
Article Type:	Paper
Date Submitted by the Author:	09-Mar-2016

Complete List of Authors:	Audran, Gérard; university of Aix-Marseille, Chemistry bosco, lionel; university of Aix-Marseille, Chemistry Nkolo, paulin; Aix-Marseille Université, Chemistry Bikanga, raphael; Université des Sciences et Technique de Masuku, Laboratoire de Substances Naturelles et des Syntheses Organometalliques Brémond, Paul; Aix-Marseille Université, Chemistry butscher, teddy; Aix-Marseille Université, Chemistry Marque, Sylvain; Aix-Marseille Université and CNRS, ICR UMR 7273

Journal Name

ARTICLE

β-Phosphorus Hyperfine Coupling Constant in Nitroxides: 6. Solvent Effect in Non-Cyclic Nitroxides

Received 00th January 20xx,
Accepted 00th January 20xx

DOI: 10.1039/x0xx00000x

www.rsc.org/

Gérard Audran,[a]* Lionel Bosco,[a] Paulin Nkolo,[a] Raphael Bikanga,[b] Paul Brémond,[a]* Teddy Butscher,[a] and Sylvain R. A. Marque,[a,c]*

In two recent articles (*Org. Biomol. Chem.* **2015** and **2016**), we showed that changes in the phosphorus hyperfine coupling constant a_P at position β in β-phosphorylated nitroxides can be dramatic. Such changes were applied to the titration of water in organic solvent and conversely of organic solvent in water. One of the molecules tested was a non cyclic nitroxide meaning that a thorough investigation of the solvent effect on the EPR hyperfine coupling constant is timely due. In this article, we show that the a_P of persistent non-cyclic β-phosphorylated nitroxides decrease with the normalized polarity Reichardt's constant E_T^N. Koppel-Palm and Kalmet-Abboud-Taft relationships were applied to get deeper insight into the effects influencing a_N and a_P: polarity/polarizability, Hydrogen Bond Donor property, and *structuredness* of the cybotactic region.

Introduction

Persistent nitroxides[1,2] are generally used in biology, as pH-probes[3] or spin probes,[4] in spectroscopy, as agents for Dynamic Nuclear Polarization enhanced Nuclear Magnetic Resonance (DNP-NMR),[5,6] or in material sciences for organic magnetic materials.[7]

The success of the application of these nitroxides relies mainly on the nitrogen hyperfine coupling constant a_N which is the cornerstone of most of these applications. The solvent effects in the cybotactic region have been investigated for several models.[8-11] It was observed that a_N increased when increasing the normalized solvent-polarity Reichardt's constant E_T^N, as exemplified with **1•** (Figure 1).[12] It was reported that the hyperfine coupling constants (hcc) of hydrogen and of fluorine atoms at position β, a_H[9] and a_F,[10] are weakly sensitive to the polarity of the solvent as well as to the temperature. In 1976, a dramatic change Δa_P in the phosphorus hyperfine coupling constants a_P with $E_{T(30)}$ (Δa_P of ca. 20 G between *n*-hexane and water) in nitroxide **2•** (Figure 1) was observed by Il'Yasov and coll.[11,#] On the other hand, with the persistent[13] *N*-(2-methylpropyl)-*N*-(1-diethylphosphono-2,2-dimethylpropyl)-*N*-oxyl radical (**3•** in Figure 1) we[14,15] recently showed that a_P was weakly sensitive to E_T^N, with a lot of outliers for alcoholic solvents and water. We also reported[16] a non linear variation in a_P with E_T^N for the stable nitroxide **2'•** and applied it to the titration of water traces in organic solvents. In 1999, Janzen and coll.[17] reported a similar effect with β-phosphorylated cyclic nitroxides (only 3 solvents were investigated). Recently, we reported an investigation on a large series (13 molecules) of β-phosphorylated pyrrolidin-based nitroxides.[18] Using the Heller-McConnell relationship[19§,¥,‡] (eq. 1 and Figure 2) applied to a_P, we showed that polarity, hydrogen bonding donor properties and the size of solvent played a role in the changes of a_P.[15,18]

$$a_P = B_0 \cdot \rho_N^\pi + B_1 \cdot \rho_N^\pi \cdot \cos^2\theta \qquad (1)$$

Taking into account the importance of non-cyclic nitroxides carrying a hydrogen atom at position β for the Nitroxide Mediated Polymerization[20,21] as well as their potential use to probe the presence of water in organic solvents,[16,22] several non-cyclic nitroxides of this family and carrying alkylcarbonyloxy groups at position β were prepared (Figure 1). Some examples of the solvent effect on the EPR pattern of signal are displayed in Figure 3 for **4•** and **5•**.

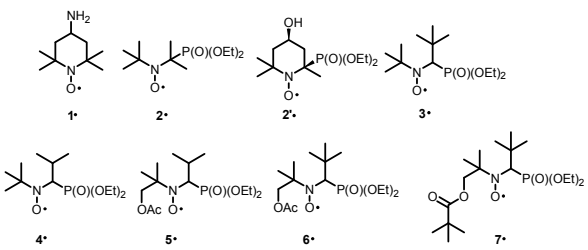

Figure 1. Nitroxides investigated.

[a] *Aix-Marseille Université, CNRS-UMR 7273, ICR, case 541, Avenue Escadrille Normandie-Niemen, 13397 Marseille Cedex 20 France.*
[b] *Université des Sciences et Technique de Masuku, Laboratoire de Substances Naturelles et des Syntheses Organometalliques, B.P. 493 Franceville, Gabon*
[c] *N. N. Vorozhtsov Novosibirsk Institute of Organic Chemistry SB RAS, Pr. Lavrentjeva 9, 630090 Novosibirsk, Russia..*
[d] ** to whom the correspondence should be sent: paul.brémond@univ-amu.fr, sylvain.marque@univ-amu.fr, g.audran@univ-amu.fr*
[e] *Electronic Supplementary Information (ESI) available: Table 1SI for the solvent parameters.Table 2SI for the KP correlations with aN. Table 3SI for the KP correlations with aP. Table 4SI for the KAT correlations with aN. table 5Si for the KAT correlations with aP. Figure 1SI for KP plots of **5•**. Figure 2SI and 3SI for KAT plots of **7•**. See DOI: 10.1039/x0xx00000x*

Table 1. Nitrogen and phosphorus hyperfine coupling constants a_N and a_P[a] in various solvents for nitroxides **1•**-**7•**.

entry	solvent[b]	**1•**[c]	**2•**[d]		**3•**[e]		**4•**		**5•**		**6•**		**7•**			
		a_N	a_N	a_P	a_N	a_P	a_N	a_P	a_N	a_P	a_N	a_P	a_N	a_P	E_T^N	c
1	pentane	15.15			13.54	46.19	13.48	49.42	13.48	49.00	13.61	45.67	13.43	44.91	0.009	205
2	*n*-hexane	15.22	14.80	40.80	-[f]	-[f]	13.58	49.68	13.48	49.00	13.49	45.55	13.43	44.79	0.009	225
3	CHex	15.19	-[f]	-[f]	13.54	46.10	13.58	49.29	13.58	48.81	13.49	45.42	13.43	44.68	0.006	285
4	octane	15.22	-[f]	-[f]	13.50	46.20	13.77	49.58	13.38	48.71	13.49	45.55	13.54	44.91	0.012	231
5	benzene	15.53	14.40	35.80	13.74	45.14	13.96	49.00	13.77	47.85	13.61	44.68	13.54	43.87	0.111	353
6	toluene	15.46	14.40	36.60	-[f]	-[f]	13.67	48.72	13.58	48.04	13.61	44.8	13.54	44.10	0.099	337
7	*t*-BuPh	15.47	-[f]	-[f]	13.70	45.70	13.77	49.10	13.58	48.24	13.49	45.05	13.54	44.44	0.099	337
8	PhBr	15.57	-[f]	-[f]	-[f]	-[f]	13.86	48.24	13.77	47.27	13.74	44.18	13.66	43.52	0.182	
9	Pyridine	15.66	14.90	32.00	13.86	44.49	13.96	48.24	13.86	46.98	13.61	43.69	13.89	43.06	0.302	466
10	AcPh	15.64	-[f]	-[f]	-[f]	-[f]	13.96	48.43	13.86	47.27	13.61	44.06	13.66	43.29	0.306	456
11	tBuPH/CH_2Cl_2	15.61	-[f]	-[f]	13.90	44.70	13.96	47.75	13.77	46.5	13.74	43.94	13.68	43.29		
12	CH_2Cl_2	15.77	-[f]	-[f]	13.90	44.61	14.15	47.66	13.96	46.31	13.74	43.69	13.74	42.95	0.309	414
13	DCE	15.71	-[f]	-[f]	13.90	45.10	14.06	47.75	13.77	46.21	13.74	43.69	13.77	42.94	0.327	400
14	$CHCl_3$	15.77	-[f]	-[f]	13.98	45.46	14.25	48.04	13.86	46.69	13.86	44.67	13.77	43.75	0.259	362
15	CCl_4	15.40	14.70	38.20	-[f]	-[f]	13.77	49.20	13.67	48.52	13.61	45.55	13.54	44.79	0.052	310
16	DME	15.27	-[f]	-[f]	-[f]	-[f]	13.96	49.00	13.77	47.75	13.61	44.69	13.54	43.98	0.231	307
17	Et_2O	15.24	-[f]	-[f]	-[f]	-[f]	13.77	49.20	13.58	48.43	13.49	45.17	13.54	44.56	0.117	251
18	*i*-Pr_2O	15.23	-[f]	-[f]	13.62	45.82	13.58	49.10	13.48	48.43	13.61	45.30	13.54	44.68	0.105	
19	*n*-Bu_2O	15.36	-[f]	-[f]	13.50	46.00	13.77	49.20	13.58	48.33	13.49	45.30	13.54	44.68	0.071	251
20	Me*t*-BuO	15.32	-[f]	-[f]	13.62	45.74	13.67	49.20	13.67	48.33	13.61	45.17	13.54	44.44	0.124	
21	14D	15.45	-[f]	-[f]	13.78	45.31	13.86	48.62	13.77	47.47	13.61	44.55	13.66	43.75	0.164	388
22	THF	15.47	14.80	35.90	13.70	45.59	13.77	49.00	13.77	48.24	13.61	44.68	13.66	44.10	0.207	359

23	AcOEt	15.60	[f]	[f]	13.66	45.66	13.77	48.91	13.67	47.85	13.61	44.93	13.54	44.21	0.228	331
24	acetone	15.62	[f]	[f]	13.82	45.42	13.86	48.91	13.77	47.47	13.74	44.55	13.77	43.87	0.355	488
25	ACN	15.76	15	31	13.86	44.73	14.06	48.04	13.96	46.5	13.74	43.81	13.77	42.94	0.46	581
26	$MeNO_2$	15.86	16	28.6	13.94	44.45	14.06	47.75	13.96	46.12	13.86	43.56	13.89	42.71	0.481	669
27	DMSO	15.77	[f]	[f]	13.8	45.40	14.06	48.91	13.96	47.27	14.73	43.69	13.77	43.29	0.444	708
28	F	16.2	[f]	[f]	14.4	43.70	14.53	47.37	14.44	44.67	14.11	42.2	14.24	40.97	0.775	1568
29	NMF	15.77	[f]	[f]	14.1	44.20	14.15	47.08	14.06	45.06	13.99	42.7	14.00	41.67	0.722	910
30	DMF	15.67	14.8	32	13.9	45.50	13.96	49.00	13.86	47.37	13.74	44.31	13.77	43.4	0.386	581
31	MeOH	16.2	15.7	21.9	14.1	45.70	14.15	48.23	14.15	46.12	13.86	43.94	13.89	43.06	0.762	858
32	EtOH	16.08	15.6	24	14	45.80	14.25	48.81	14.06	46.5	13.74	44.31	13.86	43.56	0.654	676
33	TFE	16.78	[f]	[f]	14.7	46.30	14.92	48.62	14.54	46.02	14.36	44.43	14.24	43.06	0.898	573
34	*i*-PrOH	16.04	15.2	27.6	13.94	45.94	14.15	48.91	13.86	46.89	13.74	44.68	13.77	43.98	0.546	558
35	*n*-BuOH	16.038	15.4	24.8	[f]	[f]	14.06	48.43	13.96	46.69	13.74	44.43	13.77	43.52	0.586	485
36	*t*-BuOH	15.91	[f]	[f]	13.9	46.50	14.06	49.10	13.77	47.37	13.74	45.17	13.54	44.21	0.389	467
37	BnOH	16.286	[f]	[f]	[f]	[f]	14.25	48.52	14.06	46.5	13.86	44.06	13.89	43.17	0.608	
38	EG	16.3	[f]	[f]	13.74	45.54	14.35	48.43	14.25	46.11	14.11	43.91	14.12	42.71	0.79	1050
39	TEG	15.3	15.5	22.9	13.62	45.42	14.15	48.52	13.96	46.89	13.99	44.43	13.89	43.29	0.682	
40	water/MeOH	16.72	[f]	[f]	14.5	45.70	14.83	48.81	14.54	45.83	14.23	43.81	14.35	42.59	0.71	
41	water	16.99	16.5	22.8	14.9	45.60	15.21	48.91	14.82	45.54	14.73	43.69	14.7	42.36	1	2294
42	buffer	[f]	[f]	[f]	[f]	[f]	15.12	48.91	14.83	45.54	[f]	[f]	[f]	[f]	--	--
43	AcOH	16.189	[f]	[f]	[f]	[f]	14.44	48.81	14.15	46.69	13.86	44.93	13.77	43.98	0.648	357
44	Et_3N	15.32	[f]	[f]	13.58	46.10	13.48	49.1	13.58	44.96	13.61	45.42	13.54	44.79	0.043	
45	*i*-Pr_2NH	15.36	[f]	[f]	13.62	45.91	14.15	48.67	13.58	45.54	13.49	45.3	13.66	44.79	0.145	314
46	*i*-PenOH	15.961	[f]	[f]	[f]	[f]	[f]	[f]	[f]	[f]	[f]	[f]	[f]	[f]	0.565	
47	CS_2	15.374	[f]	[f]	[f]	[f]	[f]	[f]	[f]	[f]	[f]	[f]	[f]	[f]	0.065	412
48	Mecyc	[f]	14.5	39.8	[f]	[f]	[f]	[f]	[f]	[f]	[f]	[f]	[f]	[f]		
49	PhCl	15.563	[f]	[f]	[f]	[f]	[f]	[f]	[f]	[f]	[f]	[f]	[f]	[f]	0.108	383

[a] a_N and a_P given in G.

[b] CHex: *cyclo*hexane, *t*-BuPh: *tert*-butylbenzene, PhBr: bromobenzene, AcPh: acetophenone, DCE: 1,2-dichloroethane, DME: 1,2-dimethoxyethane, 14D: 1,4-dioxane, THF: tetrahydrofurane, AcOEt: ethyl acetate, ACN: acetonitrile, DMSO: dimethylsulfoxide, F: formamide, NMF: *N*-methylformamide, DMF: *N,N*-dimethylformamide, TFE: 2,2,2-trifluoroethanol, EG: ethylene glycol, TEG: triethylene glycol, AcOH: acetic acid, *i*-PenOH: *iso*-pentanol, Mecyc: methylcyclopentane, PhCl: chlorobenzene.

c See refs. 8 and 14. d See ref. 11. e See refs. 14 and 15. f Not available.

Journal Name

ARTICLE

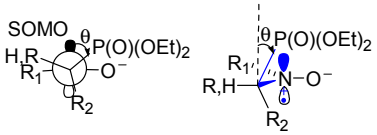

Figure 2. Hyperconjugation effect describing the origin of the coupling between the nuclear spin of the phosphorus atom and the SOMO of the nitroxyl moiety. Newman projection on the left, dihedral angle θ (in blue) on the Cram projection on the right.

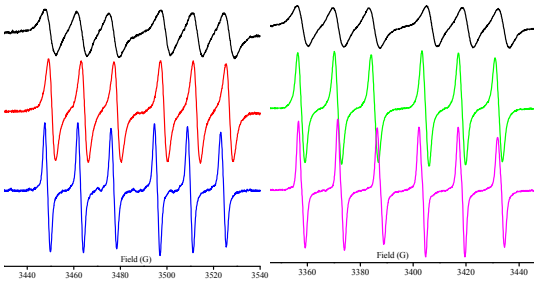

Figure 3. EPR signal of **4•** in *n*-hexane, acetonitrile, and NMF (left and top to bottom) and of **5•** in *n*-hexane, pyridine, and water (right and top to bottom)

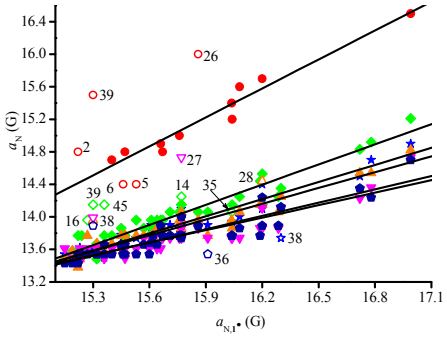

Figure 4. Correlations $a_{N,1•}$ vs a_N for **2•** (●), **3•** (★), **4•** (◆), **5•**(▲), **6•** (▼),and **7•** (⬟). Empty symbols are for outliers.

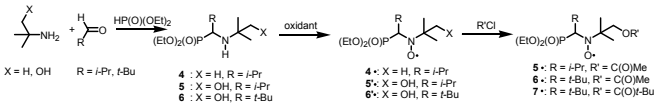

Scheme 1. Preparation of nitroxides **4• - 7•**.

Results

Preparation of nitroxides 4•-7•.

The aminophosphonates **4** - **6** were prepared in a one-pot reaction in good yield and were oxidized using oxone as oxidant in their corresponding nitroxides **4•**, **5'•** and **6'•** (Scheme 1). The esterification of the alcohol function was performed using standard procedures in good yields.

EPR analysis.

All nitroxides displayed in Figure 1 exhibit the expected 6-line EPR signal due to the coupling between the nuclear spins of the nitrogen atom (I_N = 1) and phosphorus atom (I_P = ½) and the odd electron on the nitroxyl moiety (Figure 3). Signals were recorded in more than 40 solvents. Nitrogen and β-phosphorus hyperfine coupling constants (hcc) a_N and a_P for **4•** – **7•** are collected in Table 1.

Non-specific properties of the solvent.

Among the non-specific solvent properties available – dipolar moment μ, relative permitivity constant ε_r, viscosity η and refractive index *n* –, only μ and ε_r were tested, as they were related to the polarity of the solvent (Table 1SI). As already reported for **1•**,[14] scattered plots were observed with μ and ε_r, vs a_N and a_P for **4•** - **7t•** (Figure 1SI).† Nevertheless, two trends were observed: a_N increased with increasing μ and ε_r, i.e., with increasing polarity, and a_P decreased with increasing μ and ε_r.

Correlation of a_N and a_P with benchmark hccs.

As **1•** was the nitroxide used in the first extensive study of solvent effects,[8] its a_N values are considered as benchmark values to investigate the solvent effect. Thus, a_N values were compared to those of **1•** (eq. 2).[1,2] Although **2•** was used in the first extensive solvent study (18 solvents) for nitroxides carrying a phosphorus atom at position β,[11] **3•** was used as benchmark (eqs. 3 - 5) because of its larger set of data, of its structure closer to that of **4•**-**7•**, and of its importance for NMP .

$$a_N = y_0 + \alpha_1 \cdot a_{N,1•} \quad (2)$$

Good correlations (Table 2 and Figure 4) are observed for **2•** and **4•** (5 outliers each), for **3•** and **5•**, and moderate for **6•** and **7•**. TEG is an outlier for **2•**, **4•** - **7•**, likely due to its H-bonding property and high viscosity.

$$a_N = y_0 + \alpha_2 \cdot a_{N,3•} \quad (3)$$

Very good correlations (Table 3 and Figure 5) are observed for **4•**-**7•** with a few outliers. EG (38) and TEG (39) are outliers for all nitroxides. This might be due to their H-bonding property and high viscosity.

$$a_P = y_0 + \alpha_3 \cdot a_{N,3•} \quad (4)$$

Moderate correlations (Table 4 and Figure 6) are observed with more than 15 outliers for each nitroxide. This means that the change in spin density ρ reported in a_N has a lower impact than the change in dihedral angle θ (eq. (1)).

Journal Name

ARTICLE

Table 2. Linear relationships $a_N = f(a_{N,1\bullet})$ for **2•** - **7•** in various solvents (eq. 2).

equation	nitroxide	slope α_1	error[a]	*y*-intercept	error[a]	R^{2b}	N^c	outliers
(2a)	**2•**	1.19	9	-3.65	140	0.96	10	2,5,6,26,39
(2b)	**3•**	0.70	4	2.83	56	0.92	33	38
(2c)	**4•**	0.83	3	1.00	54	0.94	36	14,16,35,39,45
(2d)	**5•**	0.65	3	3.68	51	0.90	42	28,39
(2e)	**6•**	0.51	4	5.68	60	0.81	42	27,39
(2f)	**7•**	0.55	4	5.17	58	0.85	42	36,39

[a] Error given on the last digit. [b] Square of the regression coefficient. [c] Number of data.

Table 3. Linear relationships $a_N = f(a_{N,3\bullet})$ for **4•** - **7•** in various solvents (eq. 3).

equation	nitroxide	slope α_2	error[a]	*y*-intercept	error[a]	R^{2b}	N^c	outliers
(3a)	**4•**	1.22	5	-3.00	66	0.96	25	4,19,38,39,45
(3b)	**5•**	0.96	5	0.49	62	0.94	32	38,39
(3c)	**6•**	0.79	4	2.78	52	0.94	31	27,38,39
(3d)	**7•**	0.81	5	2.52	65	0.90	32	38,39

[a] Error given on the last digit. [b] Square of the regression coefficient. [c] Number of data.

Table 4. Linear relationships $a_P = f(a_{N,3\bullet})$ for **4•** - **7•** in various solvents (eq. 4).

equation	nitroxide	slope α_3	error[a]	*y*-intercept	error[a]	R^{2b}	N^c	outliers
(4a)	**4•**	-3.62	37	98.44	513	0.81	25	28,31-36,40,41
(4b)	**5•**	-5.05	37	117.00	510	0.89	27	33,38-42,44,45
(4c)	**6•**	-4.16	0.32	100.67	440	0.89	26	14,31-34,36,40,41
(4d)	**7•**	-4.84	0.25	110.37	350	0.94	24	14,31-34,36,38-41

[a] Error given on the last digit. [b] Square of the regression coefficient. [c] Number of data.

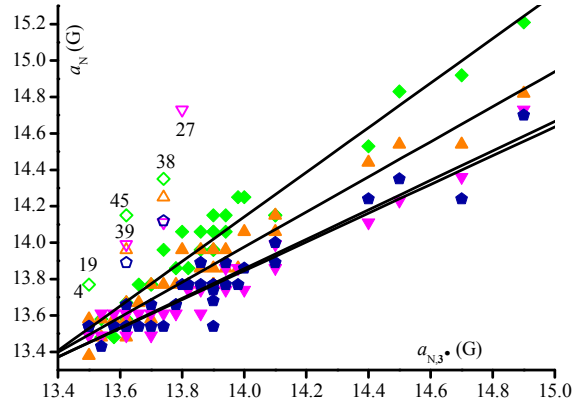

Figure 5. Correlations $a_{N,3\bullet}$ vs a_N for **4•** (◆), **5•**(▲), **6•** (▼),and **7•** (⬟). Empty symbols are for outliers.

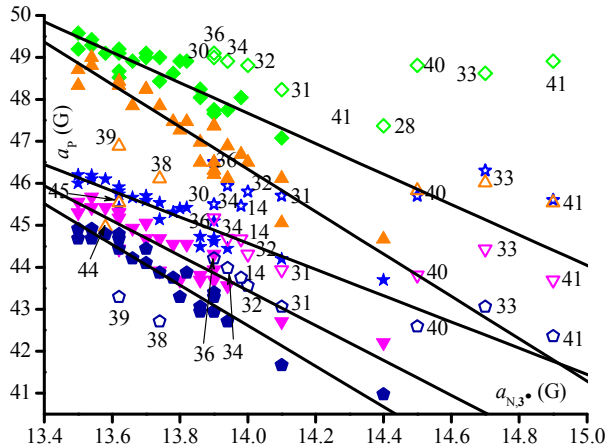

Figure 6. Correlations $a_{N,3\bullet}$ vs a_P for 3• (★), **4•** (◆), **5•**(▲), **6•** (▼),and **7•** (⬟). Empty symbols are for outliers.

$$a_P = y_0 + \alpha_4 \cdot a_{P,3\bullet} \quad (5)$$

Good correlations (Table 5 and Figure 7) are observed with more than 15 outliers for each nitroxide. This means the effects ruling **3•** are different in type and in intensity from those ruling **4•**-**7•**.

Journal Name

ARTICLE

Table 5. Linear relationships $a_P = f(a_{P,3\bullet})$ for **4•** - **7•** in various solvents (eq. 5).

equation	nitroxide	slope α_4	error[a]	*y*-intercept	error[a]	R^{2b}	N^c	outliers
(5a)	**4•**	1.03	8	1.82	352	0.89	26	5,9,13,14,28,31,33,36
(5b)	**5•**	1.70	9	29.53	413	0.96	20	9,13,14,31-34,36,38-41,44,45
(5d)	**6•**	1.29	7	-13.83	303	0.94	24	27,31-34,36,38-41
(5e)	**7•**	1.42	10	-21.03	443	0.90	26	31-34-36,38,40,41

[a] Error given on the last digit. [b] Square of the regression coefficient. [c] Number of data.

Table 6. Correlations for a_N vs E_T^N for **1•** - **7•** in various solvents (eq. (6)).

Eq.	Nitroxide	Slope α_5	Error[a]	y-intercept	Error[a]	R^{2b}	N^c	outliers	σ_I^d	E_s^e
(6a)	**1•**	1.55	8	15.20	3	0.95	43	16,29,39	-0.06	-4.20
(6b)	**2•**[f]	2.12	15	14.16	8	0.96	12	2,15,26	0.27	-5.00
(6c)	**3•**	1.11	9	13.49	4	0.85	31	38,39	0.28	-8.22
(6d)	**4•**	1.30	8	13.56	3	0.88	35	40	0.28	-7.13
(6e)	**5•**	1.03	7	13.49	3	0.85	43	no	0.48	-8.12[g]
(6f)	**6•**	0.80	7	13.47	3	0.76	42	27	0.48	-9.20[g]
(6g)	**7•**	0.85	7	13.45	3	0.79	43	no	0.48	-9.20[h]

[a] Error given on the last digit. [b] Square of the regression coefficient. [c] Number of data. [d] σ_I are estimated as recommended in ref. 23 using $\sigma_{I,Me} = \sigma_{I,i\text{-}Pr} = \sigma_{I,t\text{-}Bu} = -0.01$, $\sigma_{I,H} = 0$, $\sigma_{I,P(O)(OEt)2} = 0.32$, $\sigma_{I,CH2CO2Me} = 0.19$ see ref. 24. [e] E_s values are estimated as recommended in ref. 25 using $R_{Me} = 0$, $R_{i\text{-}Pr} = -0.76$, $R_{t\text{-}Bu} = -2.44$, $R_{P(O)(OEt)2} = -1.22$, $R_{CH2OMe} = -1.52$ see refs. 25 and 26. [f] Not reported in Figure 8. For an example see ref. 14 and 15. [g] Assuming that the CH_2OMe group cannot be smaller than the CH_2OAc group. [h] Assuming that the CH_2OMe group cannot be smaller than the CH_2OPiv group.

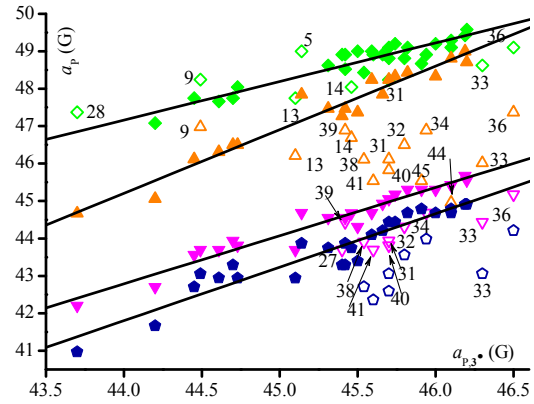

Figure 7. Correlations $a_{P,3\bullet}$ vs a_P for **4•** (◆), **5•**(▲), **6•** (▼),and **7•** (⬟). Empty symbols are for outliers

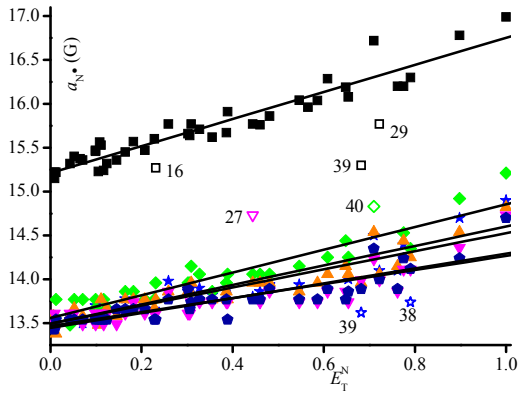

Figure 8. Correlations E_T^N vs a_N for **1•** (■), **3•** (★), **4•** (◆), **5•**(▲), **6•** (▼),and **7•** (⬟). Empty symbols are for outliers.

At first, solvent effect is investigated on a_N (eq. 6) and a_P (eq.) using the Dimroth-Reichardt solvent effect constant E_T^N.

$$a_N = y_0 + \alpha_5 \cdot E_T^N \quad (6)$$

Moderate correlations (Table 6 and eq. 6) are observed except that only a few outliers are reported and even no outliers for **5•** and **6•**. Statistics are not significantly improved by removing more data.

$$a_P = y_0 + \alpha_6 \cdot E_T^N \quad (7)$$

Moderate to good correlations (Table 7 and eq.) are observed except that more than 10 outliers are required for **3•** - **7•**. Obviously, the composite parameter E_T^N (vide infra) is not suitable to describe the solvent effect for nitroxides **3•** - **7•**.

Journal Name

ARTICLE

Table 7. Correlations for a_P vs E_T^N for **2•** - **7•** in various solvents (eq. 7)

eq.	nitroxide	Slope α_6	error[a]	*y*-intercept	error[a]	R^{2b}	N^c	outliers
(7a)	**2•**	-23.84	111	39.73	49	0.98	15	41
(7b)	**3•**	-3.02	18	46.17	6	0.88	19	5,9,12,27,30,34,36,38-41
(7c)	**4•**	-2.88	26	49.30	8	0.85	24	2,4,12,13,24,27,30-41,43
(7d)	**5•**	-3.26	14	48.77	7	0.94	31	8,9,12-14,21,25,26,28,29,44,45
(7e)	**6•**	-4.10	21	45.58	6	0.94	26	8,9,12,13,30-41,43
(7f)	**7•**	-4.61	30	44.90	9	0.88	31	31-41,43

[a] Error given on the last digit. [b] Square of the regression coefficient. [c] Number of data

Table 8. a_{Pmax} and the corresponding a_N, $a_{P,min}$ and the corresponding a_N, dihedral angle θ_1, θ_{max} and the difference $\Delta\theta$ in their corresponding solvents for nitroxides **2•** - **7•**.

nitroxide	solvent	$a_{P,max}$ (G)	a_N (G)	θ_1 (°)[a]	solvent	$a_{P,min}$ (G)	a_N (G)	θ_{max} (°)	$\Delta\theta$ (°)[b]
2•	*n*-hexane	40.80	14.80	34	MeOH	21.90	16.20	54	20
3•	*n*-pentane	46.29	13.54	28	Formamide	43.70	14.40	33	5
4•	*n*-hexane	49.68	13.58	24	NMF	47.08	14.15	29	5
5•	*n*-hexane	49.00	13.48	24	water	45.54	14.82	33	9
6•	*n*-pentane	45.67	13.48	28	Formamide	42.20	14.11	34	6
7•	*n*-pentane	44.91	13.61	27	Formamide	40.97	14.24	36	9

[a] θ_1 corresponds to θ_{min}. [b] $\Delta\theta = \theta_{max} - \theta_{min}$.

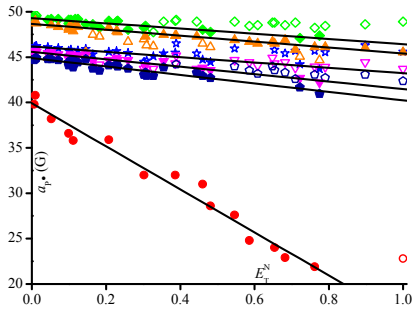

Figure 10. Correlations E_T^N vs a_P for **2•** (●), **3•** (★), **4•** (◆), **5•**(▲), **6•** (▼), and **7•** (⬟). Empty symbols are for outliers.

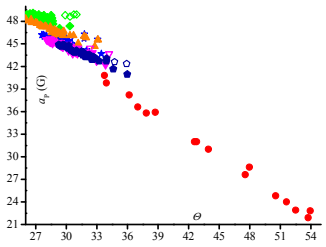

Figure 9. Plots θ vs a_P for **2•** (●), **3•** (★), **4•** (◆), **5•**(▲), **6•** (▼),and **7•** (⬟). Empty symbols are for outliers.

One way to probe the impact of conformational changes on a_P is to determine the dihedral angle θ between the C—P bond and the p-shape orbital on the N-atom of the nitroxyl moiety as given in eq. (1). However, this requires to know the values of $\rho_N^{\pi}B_1$ which depend on the value of ρ_N^{π}, the latter being solvent dependent as θ is. Nevertheless, $\rho_N^{\pi}B_1$ is known in non polar solvents for nitroxides carrying diethoxyphoshonyl group and commonly accepted as $\rho_N^{\pi}B_1$ = 59 G. As ρ_N^{π} is proportional to a_N, the ratio $a_{P,non\ polar\ solvent}/a_{P,n}$ (eq. 8) affords the value of θ for each solvent and, hence, an insight into the solvent dependence of the conformation. Moreover, it was assumed $\rho_N^{\pi}B_1$ = 59 G for nitroxides **3•** to **7•**, due to their small difference in a_N, as well as for **2•**.

$$\frac{a_{P,1}}{a_{P,n}} = \frac{a_{N,1}}{a_{N,n}} \cdot \frac{\cos^2\theta_1}{\cos^2\theta_n} \qquad (8)$$

Values of $a_{P,max}$ are in the same type of solvent, i.e., *n*-hexane or *n*-pentane whereas solvents are different for $a_{P,min}$, i.e., formamide for **3•**, **5•** and **7•**, water, for **5•**, NMF for **4•** and MeOH for **2•** (Table 8). The type of nitroxide has no influence on the values of a_N corresponding to $a_{P,max}$ and $a_{P,min}$. On the other hand, $a_{P,max}$ and $a_{P,min}$ are split in 3 groups, one for **2•** (lowest $a_{P,max}$ and $a_{P,min}$), one for **3•**, **6•**, and **7•** (medium a_P values) and one for **4•** and **5•**, in good agreement with the structural differences, *t*-Bu group for **3•**, **6•** and **7** • vs *i*-Pr group for **4•** and **5•** (Figure 1). Nevertheless, due to a change in dihedral angle $\Delta\theta$ of 5° - 9° **3•** - **7•** are gathered in the same family exhibiting highly restricted motion and very different from **2•** ($\Delta\theta$ = 20°).

Journal Name

ARTICLE

Multiparameter correlations.

As several outliers were observed for the plots a_N vs E_T^N and a_P vs E_T^N, multi-parameter relationships based on the Koppel–Palm (KP, eqs. **(**9) and (10)) and the Kalmet–Abboud–Taft (KAT, eqs. (14) and (15)) relationships were tested with a_N and a_P. The 6-parameter KP relationship combines two non-specific parameters – the polarizability parameter given by the Lorenz-Lorentz function (eq. 11) with the refractive index *n*, and the polarity parameter given by the Kirkwood function (eq. 12) with the relative permittivity ε_r, – and four solvent specific parameters: the solvent basicity/nucleophilicity parameter *B*, the solvent acidity/electrophilicity parameter *E*, the Hildebrand's solubility parameter δ_H, and the molar volume V_M of the solvent. The values of *E* were given by eq. (13) and using the Dimroth-Reichardt polarity parameter $E_{T,30}$.

$$\log a_N = \log a_{N,0} + a_1 \cdot f(n^2) + a_2 \cdot f(\varepsilon_r) + a_3 \cdot B + a_4 \cdot E + a_5 \cdot \delta_H^2 + a_6 \cdot V_M \quad (9)$$

$$\log a_P = \log a_{P_0} + b_1 \cdot f(n^2) + b_2 \cdot f(\varepsilon_r) + b_3 \cdot B + b_4 \cdot E + b_5 \cdot \delta_H^2 + b_6 \cdot V_M \quad (10)$$

$$f(n^2) = \frac{(n^2 - 1)}{(n^2 + 2)} \quad (11)$$

$$f(\varepsilon_r) = \frac{(\varepsilon_r - 1)}{(2\varepsilon_r + 1)} \quad (12)$$

$$E = E_{T,30} - 25.10 - 14.84 \cdot f(\varepsilon_r) - 9.59 \cdot f(n^2) \quad (13)$$

Whatever the combination of parameters – from one to six parameters – applied to the KP relationship (eq. 9) the basicity *B*, the molecular volume V_M and the polarizability $f(n^2)$ are useless to describe the effect of the solvent on a_N, except for **1•** for which a correlation is observed (eq. 9a) with *E* and $f(n^2)$. For **2•**, only *E* is sufficient to describe the effect of the solvent (the occurrence of the polarizability $f(n^2)$ is 84% reliable, below the conventional statistical requirements (eq. 9b in Table 9). For **3•** - **7•**, a_N values are nicely described by a combination of *E* and *c* parameters, e.g., no outliers for **5•** and **7•**. Nevertheless, nice correlations (see Table 2SI and Figure 1SI) are also observed with $f(\varepsilon_r)$ and *c* except for **6•** (no correlation). Whatever the parameters, $CHCl_3$ (14), TFE (33), EG (38), TEG (39) and AcOH (43) were the most frequent outliers. At this time, there is no rationale for this observation.

Whatever the combination of parameters – from one to six parameters[27,28] – applied to the KP relationship (eq. 10), the basicity *B*, the acidity *E*, and polarizability $f(n^2)$ are useless to describe the effects of the solvent on a_P (very poor statistical outputs). Surprisingly, the changes in a_P of **2•** - **4•** with the solvent cannot be described by eq. (10). Interestingly, a_P for **5•** - **7•** (Table 10) are described by a 3 parameter KP relationship: $f(\varepsilon_r)$ (polarity), *c* (cohesive pressure), and V_M (molar volume). Indeed, good statistical outputs are obtained with two parameters ($f(\varepsilon_r)$ and *c*, see Table 3SI) but the scattering decreases when V_M is included (Figure 2SI). Water (41) and Et_3N (44) are the only outliers observed for KP relationships relying on $f(c,f(\varepsilon_r))$ or $f(c,f(\varepsilon_r),V_M)$.

The KAT relationships (eqs. (14) and (15)) are also applied to describe the solvent effects on a_N and a_P using 4-5 cybotactic parameters:[12] one non specific parameter π* describing the polarity/polarizability effect, the discontinuous polarizability correction term δ, the Hydrogen Bonding Acceptor (basicity) HBA property β and the Hydrogen Bonding Donor (acidity) property α. In some cases, cohesive pressure *c* (given as δ^2_H) is included in the KAT relationship.

$$\log a_N = \log a_{N_0} + c_1(\pi^* + c_2 \cdot \delta) + c_3 \cdot \alpha + c_4 \cdot \beta + c_5 \cdot \delta_H^2 \quad (14)$$

$$\log a_P = \log a_{P_0} + d_1(\pi^* + d_2 \cdot \delta) + d_3 \cdot \alpha + d_4 \cdot \beta + d_5 \cdot \delta_H^2 \quad (15)$$

Whatever the combination of parameters – from one to five parameters – applied to the KAT relationship (eq. (14): the HBA property β and the discontinuous polarizability correction term δ are useless to describe the effects of the solvent on a_N (very poor statistical outputs). The normalized Reichardt E_T^N encompasses three effects: polarity, polarizability, and HBD property α of the solvent (eq. 16). As expected from eq. (16 and correlations $a_N = f(E_T^N)$ (Table 6), good correlations involving π* and α are obtained (Table 4SI). Nevertheless, a 3-parameter correlation using *c* affords better statistical outputs (Table 11), which is observed as a decrease in the scattering (Figures 2SI and 3SI). The use of *c* for the correlation of **4•**, **5t•**, and **7•** suppresses the outliers observed when two parameter correlations are applied.

$E_T^N = 0.36 \cdot \pi^* + 0.47 \cdot \alpha + 0.01$ (16)

Journal Name

ARTICLE

Table 9. Koppel-Palm linear correlations of a_N for **1•** - **7•** (eq. (9)).

eq.	nitroxide	*y*-intercept[a]	a_4[a,b]	a_5[a,b]	R^{2c}	N^d	*F*-test[e]	w_E[f]	w_c[f]	outliers
	1•[g]	14.82 (14)	0.056 (2)	-[h]	0.94	41	280	89	11[i]	29,39
(9a)										
	2•[j]	15.09 (44)	0.058 (6)	-[h]	0.93	15	82	86	14[i]	2,15,26
(9b)										
	3•	13.49 (2)	0.015 (4)[k]	0.0004 (1)	0.94	26	197	38	62	14,33,38,39
(9c)										
	4•	13.57 (4)	0.039 (4)	0.0002 (1)[l]	0.87	36	110	79	21	14,31,38
(9d)										
	5•	13.50 (3)	0.026 (3)	0.0002 (1)[m]	0.90	39	168	72	28	none
(9e)										
	6•	13.44 (12)	0.010 (3)	0.0004 (1)	0.89	37	140	32	68	27,33
(9f)										
	7•	13.41 (4)	0.016 (3)	0.0004 (1)	0.90	39	159	44	56	none
(9g)										

[a] Errors are given on the last digit in parentheses. [b] Student *t*-test at 99.99% unless otherwise mentioned. [c] Square of the regression coefficient. [d] Number of data. [e] Student-Fischer *F*-test given at 99.99%. [f] Weight of each parameter in percent with an error of ± 7% as given by eqs. 17 and 18. [g] Polarizability was the only other parameter affording reliable statistical outputs, i.e., a_1 = 1.61 (50) and *t* = 99.73%. [h] Not included in the correlation. [i] Given for $f(n^2)$. [j] a_1 = -2.39 (1.59) and *t*-test at 84%. Other possibilities were even worse. [k] *t*-test = 99.89%. [l] *t* = 92.87%.. [m] *t* = 99.90%.

Table 10. Koppel – Palm multiparameter correlations (eq. (10)) based on the Kirkwood function of the relative permittivity ε_r, the cohesive pressure (square of the Hildebrand solubility parameter δ_H), and on the molar volume V_M for nitroxides **5•** - **7•**.

eq	nitroxide	log$a_{P,0}$[a]	b_2[a,b]	b_5[a,b]	b_6[a,b]	R^{2c}	F^d	N^e	$w_{f(\varepsilon r)}$[f]	w_c[f]	w_{VM}[f]	outliers
(10a)	**5•**	48.5 (6)	-3.2 (11)[g]	-0.0016 (4)[h]	0.009 (4)[i]	0.80	45	38	31	42	27	41,44
(10b)	**6•**	45.4 (5)	-1.6 (9)[j]	-0.0015 (4)	0.005 (3)[k]	0.74	33	39	24	54	22	41
(10c)	**7•**	44.7 (5)	-1.5 (9)[l]	-0.0020 (3)	0.006 (3)[m]	0.81	49	39	18	60	22	41

[a] Errors are given on the last digit in parentheses. [b] Student *t*-test of confidence given at 99.99 % unless otherwise mentioned. [c] Square of the regression coefficient. [d] Student-Fischer *F*-test of reliability given at 99.99% confidence. [e] Number of data. [f] Weight of each parameter in per cent with an error of ± 7% as given by eqs. 17 and 18. [g] *t* = 99.40%. [h] *t* = 99.94%. [i] *t* = 98.4%. [j] *t* = 94.5%. [k] *t* = 98.20%. [l] *t* = 93.75%. [m] *t* = 94.70%.

Table 11. Kalmet – Aboud – Taft multiparameter correlations (eq. 14) for a_N of nitroxides **1•** - **7•** based on the polarity/polarizability parameter π*, the cohesive pressure *c*, and on the Hydrogen Bonding Donor (HBD) parameter α of solvents.

eq.	nitroxide	*y*-intercept[a]	c_1[a,b]	c_3[a,b]	c_5[a,b]	R^{2c}	F^d	N^e	w_{π^*}[f]	w_α[f]	w_c[f]	outliers
(14a)	**1•**	15.18 (3)	0.49 (6)	0.68 (4)	0.0002 (6)[g]	0.96	281	41	30	58	12	29,39
(14b)	**2•**	14.10 (19)	0.77 (35)[h]	1.01 (15)[i]	0.0002 (2)[j]	0.96	68	12	22	64	12	2,15,26
(14c)	**3•**	13.48 (4)	0.33 (8)[i]	0.44 (6)	0.0002 (1)[k]	0.93	101	28	28	49	23	38,39
(14d)	**4•**	13.56 (4)	0.38 (9)	0.44 (6)	0.0002 (1)[l]	0.87	77	40	31	49	20	none
(14e)	**5•**	13.44 (3)	0.33 (5)	0.33 (4)	0.0002 (1)	0.93	163	40	31	44	25	none
(14f)	**6•**	13.41 (3)	0.13 (5)[m]	0.13 (4)[n]	0.0004 (1)	0.90	103	38	16	20	64	27,33
(14g)	**7•**	13.38 (3)	0.23 (5)	0.18 (4)	0.0003 (1)	0.92	137	40	27	29	44	none

[a] Errors are given on the last digit in parentheses. [b] Student *t*-test of confidence given at 99.99% unless otherwise mentioned. [c] Square of the regression coefficient. [d] Student-Fischer *F*-test of reliability given at 99.99% confidence. [e] Number of data. [f] Weight of each parameter in percent with an error of ± 7% as given by eqs. 17 and 18. [g] *t* = 99.10%. [h] *t* = 94.10%. [i] *t* = 99.98%. [j] *t* = 64.00%. [k] *t* = 99.00%. [l] *t* = 98.29%. [m] *t* = 96.80%. [n] *t* = 99.60%.

Whatever the combination of parameters – from one to five parameters – applied to the KAT relationship (eq. (15)): the HBA property β and the discontinuous polarizability correction term δ are useless to describe the effects of the solvent on $a_{\beta,P}$ (very poor statistical outputs). As expected from correlations $a_P = f(E_T^N)$ and eq. (16), the polarity/polarizability π* parameter is required to describe a_P values (eq. 15 in Table 12). However, in sharp contrast to a_N values, the HBD α parameter is not

always required to describe the solvent effect, as in the case of **4•** (eqs. 15d and e), **6•** (eq. 15i), and **7•** (eq. 15k, see Table 5SI). Indeed, when α is replaced by *c*, better correlations are observed, e.g., for **6•** and for **7t•** (Figure 3SI). Interestingly, a_P of **3•** and **4•** are better described using a 3-parameter correlation: π^*, α, and *c*. In sharp contrast to KP, KAT describes all nitroxides even in the case of **4•** which exhibits 14 outliers (Table 12).

Journal Name

ARTICLE

Table 12. Kalmet – Aboud – Taft multiparameter correlations (eq. (15) for a_p of nitroxides **1•** - **7•** based on the polarity/polarizability parameter π*, the cohesive pressure *c*, and on the Hydrogen Bonding Donor (HBD) parameter α of solvents.

eq	nitroxide	*y*-intercept[a]	d_1[a,b]	d_3[a,b]	*t*[c]	d_5[a,b]	R^2[d]	*F*[e]	*N*[f]	w_{π^*}[g]	w_α[g]	w_c[g]	outliers
(15a)	**2•**	40.52 (58)	-9.87 (93)	-12.86 (63)	99.99	-[h]	0.98	297	14	34	66	-[i]	41
(15b)	**3•**	46.51 (13)	-1.34 (27)	1.19 (19)	99.99	-0.0014 (13)	0.83	36	26	31	37	32	27,30,36,41
(15c)	**4•**	49.65 (6)	-1.03 (15)	0.19 (9)	95.00	-0.0009 (2)	0.90	65	26	48	13	39	12-14,24-27,29,30,35,37-39,41
(15d)	**5•**	48.71 (8)	-1.65 (14)	-1.16 (10)	99.99	-[h]	0.94	230	32	28	72	-[i]	12-14,25,26,28,29,44
(15e)	**6•**	44.54 (10)	-1.84 (17)	0.08 (13)	49.0	-[h]	0.78	63	38	94	6	-[i]	28,29
(15f)	**7•**	55.80 (10)	-1.92 (18)	-0.25 (13)	94.0	-[h]	0.82	82	38	85	15	-[i]	28,29

[a] Errors are given on the last digit in parentheses. [b] Student *t*-test of confidence given at 99.99%. [c] Student *t*-test. [d] Square of the regression coefficient. [e] Student-Fischer *F*-test of reliability given at 99.99% confidence. [f] Number of data. [g] Weight of each parameter in percent with an error of ± 7% as given by eqs. 17 and 18. [h] Not used in the correlation. [i] Not determined.

The absolute values of the coefficients of the KP and KAT relationships describe the impact of each effect whereas the relative distribution given by their weight (*w* in %, eqs. 17 and 18) provides information on their relative importance.[29] The weight *w* (eq. 17) of each effect depends on parameter C_i and its respective weighted parameter α_i, given in eq. (18). The latter depends on the average of each parameter and on the degree of freedom (number of data *N* and number of parameters *p*, eq. 18).

$$w = \frac{\alpha_i \cdot C_i}{\sum \alpha_i \cdot C_i} \qquad (17)$$

$$\alpha_i = \sqrt{\frac{\sum_{i-1}^{N} \left(x_i - \overline{x}_i\right)^2}{N - (p-1)}} \qquad (18)$$

The significance of the parameter used was estimated with the square of the linear regression coefficient (R^2) and the Student-Fischer *F*-test of the correlation as well as the Student *t*-test, and the weighting parameter *w*.[29,30]

Discussion

General considerations on hccs.

For historical considerations,[8] a_N of **1•** are commonly accepted as the benchmark values all other a_N are compared with. As displayed in Figure 4 and Table 2, moderate correlations are reported (R^2 > 0.81) if several outliers are removed. Hence, a_N of **2•** to **7•** experienced the same effect as that experienced by a_N of **1•** but to a different extent (Table 2), as highlighted by the slopes greater than 1 for **2•**, between 0.70 – 0.83 for **3•** - **4•**, and 0.51 – 0.65 for **5•** - **7•**. Interestingly, as the polarities of **3•** and **4•** (σ_I = 0.28, see Table 6) are the same, and those for **5•** - **7•** (σ_I = 0.48, see Table 6) are the same, the increase in the slope from **4•** to **3•** and **6•**/**7•** to **5•** agrees nicely with the decrease in the steric hindrance around the nitroxyl moiety from **3•** (E_s = -8.22) to **4•** (E_s = -7.13) as well as from **6•**/**7•** (E_s = -9.20) to **5•** (E_s = -8.12). Better correlations are observed when a_N of **3•** is used as reference (Table 3 and Figure 5).

Given by the EPR theory,[19] the hyperfine coupling on position α is directly related to the electron density localized on the nucleus, and in turn to the shape of SOMO (Fermi contact term which corresponds to the electron density on the nucleus Q_N, eq. 19). That is, for π-radicals, the SOMO is of *p*-type and thus any increase in the character *s* will lead to an increase in electron density and, hence, to an increase in a_N.

$$a_X = cte \cdot Q_N \qquad (19)$$

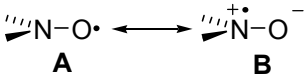

Figure 11. Mesomeric forms of the nitroxyl moiety.

In the case of nitroxides, the electron density Q_N is controlled both by the presence of electron widthdrawing groups (EWG) – which favours form **A** over form **B** (Figure 11),[6,8,9] that is, Q_N decreases, a_N decreases – and by the hybridation (pyramidalization) at the nitrogen atom, varying from sp^3 to sp^2 (Figure 12), i.e., the higher the pyramidalization (form **C**), the higher the character *s* in the SOMO, the higher a_N and conversely.

Plots a_N vs $a_{N,3•}$ are better than those reported for a_N vs $a_{N,1•}$ and afford a deeper insight into the effects ruling a_N values. That is, as **3•** and **4•** exhibit the same polarity (see Table 6),

the slope larger than 1.0 is ascribed to a smaller steric hindrance in **3•** (E_s = -8.22) than in **4•** (E_s = -7.13). The close slope for **6•** and **7•** means that the pivalate group (OPiv) is not more sterically demanding than the acetate group (OAc). The smaller slope is then ascribed to both a stronger polar effect and a larger steric hindrance around the nitroxyl moiety in **6•** and **7•** than in **3•**. This is nicely confirmed by the smaller slope for **5•** (σ_I = 0.38 and E_s = -8.13) than for **4•** (σ_I = 0.28 and E_s = -7.13). The slope for **5•** very close to 1.0 means that the destabilizing polar effect in **5•**, i.e., form **A** favoured over form **B** (Figure 11), is balanced by the release of the steric hindrance around the nitroxyl moiety, i.e., *iso*propyl group in **5•** smaller than *tertio*butyl group in **3•**, affording a better access of the solvent to the nitroxyl moiety.

The Heller-McConnel relationship (eq. 1) shows that a_P is directly proportional to the electron density ρ_N^{π},[19] which, in turn, is expected to be linearly related to a_N, implying that increasing a_P is expected with increasing a_N, provided no change in the hybridization or in the mode of solvation.[9,19] Hence, a decrease in a_P is observed with increasing a_N (Table 1) leading to scattered plots between a_P and both $a_{N,\mathbf{1}\bullet}$ (not shown) and $a_{N,\mathbf{3}\bullet}$ (Figure 6 and Table 4). Thus, a_P of **3•** was applied as reference for **4•** to **7•** (Table 5and Figure 7). Despite good correlations, the large number of outliers impedes any reliable and quantitative discussion on the slopes reported in Table 5. Nevertheless, this observation points to a conformational effect (changes in θ, eq. (1)) overmatching the increase in the spin density at the N atom (ρ_N^{π} in eq. (1)).

Correlations based on the normalized Dimroth-Reichardt constants E_T^N.

The correlations a_N with E_T^N or $E_{T(30)}$ have been known since the work of Napier et al.[8] for **1•** and that of Il'Yasov and coll.[11] for **2•**. As recently reported,[14] the lower *y*-intercept for β-phosphorylated nitroxides **2•** - **7•** than for **1•** is due to the presence of the strong EWG P(O)(OEt)$_2$ (σ_I = 0.32)[24] favouring form **A** over form **B** (Figure 11). Interestingly, **2•** - **4•** exhibit very close polarities whereas a_N of **2•** is 0.6 G higher. This denotes a stronger pyramidalization in **2•** than in **3•** and **4•**.

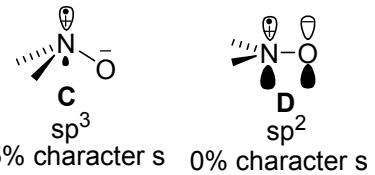

Figure 12. Canonical forms for the hybridization at the nitrogen atom of a nitroxyl moiety and % of character *s* in the SOMO

The same y-intercept for **5•** - **7•** as for **3•/4•** despite a higher polar effect in **5•** – **7•** denotes a stronger pyramidalization in **5•** - **7•** (Figure 12) than in **3•/4•**, which balances the detrimental effect of the presence of EWG, i.e., form **A** favoured over form **B**.

It has been reported that the slope from eq. (6) depends both on the steric hindrance around the nitroxyl moiety[8,15] – i.e., increasing bulkiness around the nitroxyl moiety implies lower solvation, and, in turn, lower solvent effect – and on the presence of EWG attached to the nitroxyl moiety[9,15] – i.e., the presence of EWG favours form **A** which is less sensitive to the solvent effect. The polar effect is estimated by adding the electrical Hammett constant σ_I of all the groups attached to the nitroxyl moiety, as previously reported (Table 6).[25,31] The bulkiness of the groups attached to the nitroxyl is estimated using the assumptions done and conformations observed in the case of the cross-coupling reactions between alkyl radicals and nitroxides (Table 6).[25,31] The impact of the polarity and bulkiness effect is estimated by the plots α_5 vs σ_I and α_6 vs E_s (Figure 13a and b, respectively).

$$y = 1.51(9) - 1.24(24)\cdot\sigma_I \quad (20)$$

R^2 = 0.87 N = 6 s = 0.11

$$y = 2.22(17) + 0.14(2)\cdot E_s \quad (21)$$

R^2 = 0.92 N = 6 s = 0.09

Nice correlations (eqs. 20 and 21 and Figure 13) are observed for both effects when **2•** is considered as outlier. As expected, the influence of the solvent effects on a_N (slope α_5) decreases with increasing polarity due to EWG and increasing the bulkiness of the group attached to the nitroxyl moiety.

A quick glance at the trends given by σ_I, E_s, and α_5 (Figure 14) shows that the best agreement with the experimental data (trends for α_5) is observed for the trend given by E_s provided **2•** is not included. That is, the influence of the solvent effect is stronger with decreasing bulkiness of the groups attached to the nitroxyl moiety, i.e., a better solvation of the nitroxyl moiety is observed (form **B** favoured) for an easier access. Hence, the major effect is due to the bulkiness of the group attached to the nitroxyl moiety although the presence of EWG also plays a role re-enforcing the influence of the steric effect.

Journal Name

ARTICLE

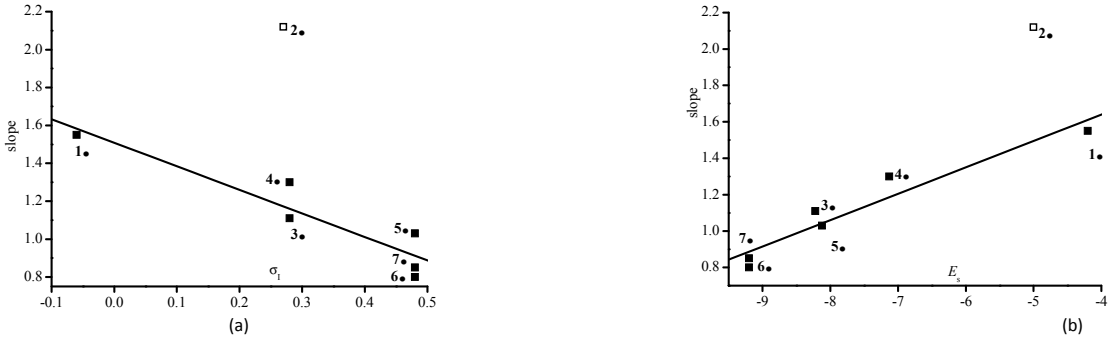

Figure 13. Plots of the slope α_5 against σ_I (a) and E_s (b). Empty symbol for outliers.

σ_I	**7• = 6• = 5• > 3• = 4• ≈ 2• > 1•**
E_s	**7• = 6• < 3• ≈ 5• < 4• < 2• < 1•**
slope a_N	**7• ≈ 6• < 5• ≈ 3• < 4• < 1• < 2•**

Figure 14. Trends in σ_I, E_s, and α_5.

Due to some freedom of motion around the C—N bond (vide infra),[11] the conformation affording the best solvent-nitroxyl moiety is always favoured, implying the discrepancies observed in the trends (Figure 14) and in the plots (Figure 13) with the steric descriptors E_s, estimated assuming a locked conformation.[25] Indeed, taking into account data from literature and a_P values, the conformation displayed in Figure 15a is the most probable for **2•** in apolar solvents as all the *syn*-1,3 interactions are minimized due to the *anti*clinal positions of all the groups. It implies one methyl group *anti* to the N—O• bond and one methyl group *syn* to the N—O• bond as well as a dihedral angle of 60°, i.e., θ = 30°, in good agreement with the experimental value (Table 8), between the C—P and N—O• bonds. Moreover, the *syn*-position of one methyl group is expected to hamper the solvation of one side of the p-orbital describing one of the oxygen lone pairs. Shifting from apolar to polar solvents moves the diethoxyphosphonyl group closer to the nitroxyl moiety, i.e., θ ≈ 60° generating strong destabilizing *syn*-1,3 interactions between methyl groups and a quasi-*syn* conformation between C—P and N—O• bonds (Figure 15b).

As such conformation is not stable, rotation around the C—N bond provides a new conformation, as displayed in Figure 15c, with all groups again in an *anti* conformation and a *gauche* conformation for the nitroxyl moiety with θ = 30°, affording a better access to the p-orbital for the solvation of the nitroxyl moiety.

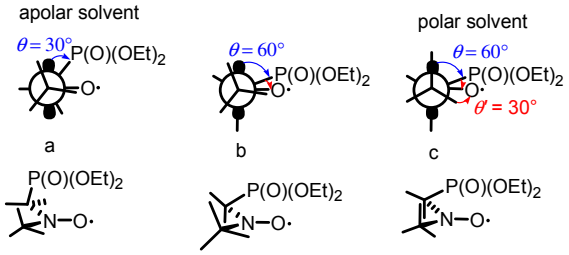

Figure 15. Newman's (top) and Cram's (bottom) projections of the most probable conformers of **2•** in apolar and polar solvents.

The *y*-intercepts for the plots a_P vs E_T^N, for E_T^N = 0, correspond to the a_P values expected in *n*-pentane and *n*-hexane. Interesting, the *y*-intercepts of the plot a_P vs E_T^N for **2•** - **7•** (Table 7and Figure 10) agree nicely with the experimental data (Table 8).

Il'Yasov and coll.[11] showed that the a_P of **2•** is temperature dependent, implying that the conformation of **2•** changes with the temperature, meaning that the rotation around the C—N bond is partly free.

Eq. (1) shows that a_P depends on both the change in spin density given by ρ_N^π and on the conformational changes given by θ, meaning either the slope in eq. (7) increases as expected with the increasing solvent polarity as form **B** is favoured over form **A**, provided no change in conformation, i.e., $\Delta\theta \approx 0°$ or the slope decreases, implying that the conformational changes, i.e., increasing θ values, overbalance the effect of the solvent polarity. Recently, we ascribed the solvent effect to a change in conformation for a negative slope. A glance at the trends given by σ_I and E_s (Figure 16) shows that these effects cannot describe the changes in a_P observed. Consequently, it is not possible to discuss quantitatively the influence of the polarity, the bulkiness, and the conformation changes on the slope.

σ_I	**7•** = **6•** = **5•** > **3•** = **4•** ≈ **2•**
E_s	**7•** = **6•** < **3•** ≈ **5•** < **4•** < **2•**
slope a_P	**4•** > **3•** > **5•** > **6•** > **7•** > **2•**

Figure 16. Trends in σ_I, E_s, and α_6.

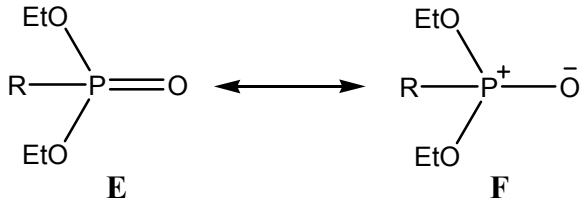

Figure 17. Mesomeric forms for the phosphoryl group.

Applying eq. (8) affords some hints on the conformational changes through the variation in dihedral angle $\Delta\theta$ (Figure 9 and Table 8). Except for **2•** for which $\Delta\theta$ = 20°, the values of $\Delta\theta$ are centred at 7°±2. In contrast with previous reports,[15,18] $\Delta\theta$ can be related neither to Δa_P nor to the slope α_6. Nevertheless, the negative slopes in eq. (7) mean that the increase in dihedral angle θ overmatches the increase in spin density ρ_N^{π} due to the increase in solvent polarity (vide supra). It is likely that the phosphoryl group is solvated in the same way for all nitroxides and the increase in polarity of the solvent favours form **F** (Figure 17).

It has been noted that increasing the polarity of the solvent favours the mesomeric forms **B** and **F** of the nitroxyl and phosphoryl moieties, respectively (Figures 11 and 17), implying that the attractive dipole-dipole interaction between the positive P- and the negative O-atoms of the phosphoryl and the nitroxyl moieties, respectively, is the driving force leading to a change in the dihedral angle θ (Scheme 2).[Ω] Such a conformation change from a non polar to a polar solvent is expected to lead ultimately to the formation of a highly strained 4-membered ring of the azaoxaphosphetane type (Scheme 2).

Multiparameter approach.

General considerations.

As mentioned above, significant scattering was observed for the plots a_N vs E_T^N and a_P vs E_T^N. It led us to investigate the solvent effect through the Linear Solvation Energy Relationship[12,32] (LSER), as given by eq. 22: A and A_0 are the values of the solvent-dependent physico-chemical properties; the polarity/polarizability terms describe the solute/solvent dipole and induced dipole interactions: given, for example, by the Kirkwood functions $f(\varepsilon_r)$ (eq. (12)), by the Lorenz-Lorentz function $f(n^2)$ (eq. (11)), or by π*; the hydrogen bonding terms describe the HBD/HBA interactions between the solvent and the solute: given for example, by α and β parameters as defined by Abraham,[12,27] or by E (electrophilicity/Lewis acidity) and B (nucleophilicity/Lewis basicity) as defined by Koppel and Palm:[33] and the bulk/cavity terms (*structuredness* of the solvent) describe the energy needed to form cavities for the solute molecules: given, for example, by the cohesive pressure c or V_M.[12,27,28] The choice of the parameters depends on the type of correlation investigated.[√]

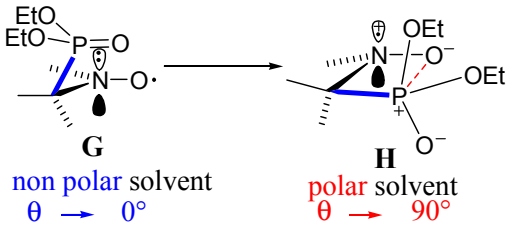

Scheme 2. Conformation change by rotation around the C—N bond from a non polar solvent to a polar solvent.

The Koppel-Palm (eqs. (9) and (10)) and the Kalmet – Abboud – Taft (eqs.(14) and (15)) relationships are the most popular approaches to describe the solvent effect in the cybotactic region with specific and non-specific parameters.[12,27,28]

$A = A_0$ + polarity/polarizability terms + hydrogen bonding terms + bulk/cavity terms (22)

Parameters $f(n^2)$, $f(\varepsilon_r)$, E, B, π*, E_T^N, α and β are currently applied to describe the solvent effect on physical constants such as spectroscopic data.[12,27,28] The use of the cohesive pressure c and the molar volume V_M is less frequent in such cases.[12] Indeed, the cohesive pressure c is related to the energy required to create cavities in a liquid in order to accommodate solute molecules during the process of dissolution.[12] How this might play a role is not so obvious. In fact, c can also be considered as a parameter describing *the stiffness of structuredness* of the solvent, i.e., the organization of the solvation cage. It is noticed that c increases with the increasing H-bonding capacity of the solvent. The molar volume V_M is often used to take into account the effect of the size of the molecules. However, the weakness of this parameter is that the molecule is described as a sphere.[27] These parameters describing the *structuredness* of the solvent are expected to play a role when a solute exhibits stereocenters and bulky groups.

Multiparameter approach. Analysis of a_N.

As mentioned above, significant scattering was observed for the plots a_N against E_T^N for several nitroxides. Thus, the very popular KP and KAP relationships were applied to get deeper insight into the effects involved in the change in a_N.[12,27,28] Nitroxides **3•** - **7•** are well described using a two-parameter KP relationships – E and c or $f(\varepsilon_r)$ and c – except for **6•**. The use of a bi-parameter equation increases the quality of the correlation (higher R^2 and good F-test, Table 9). The absolute values of the parameters provide information on the strength of the effect while the weights (distribution of the effect for each parameter) provide insight into the importance of each effect for each nitroxide. Meaningful, for **1•** and **2•**, the use of $f(n^2)$ and E (eq. 9) is expected given the good plots reported for a_N vs $E_T(30)$ and eq. (13), as E_T^N is described as a function of the polarizability $f(n^2)$, the polarity $f(\varepsilon_r)$ and the parameter E. Interestingly, taking into account the errors, c does not vary significantly with the nitroxide, meaning that the *structuredness* of the solvent in the cybotactic region is the same around the nitroxyl moiety, and its positive value implies that the higher the *structuredness*, the stronger the solvent effect. In contrast to what was shown in previous work,[18] c

plays a major role (w_c > 60%) except for **6•** (w_c = 6%). In fact, *structuredness* depends a lot on the ability of the solvent to built an H-bond network. Then, as $f(\varepsilon_r)$ describes only the polarity effect of the solvent, the impact of H-bonding in a_N is taken into account by *c*, affording slightly larger values when *E* is used. The values of *E* are gathered in 3 groups: 0.56 and 0.58 for **1•** and **2•**, respectively, 0.010 – 0.016 for **3•**, **6•**, and **7•** and 0.026 and 0.039 for **5•** and **4•**, respectively. The parameter *E* cannot be straightforwardly related to the polarity of the nitroxide. However, a trend arises: from **1•** to **2•** bulkiness and polarity increase as well as for **3•** to **6•**/**7•** and **4•** to **5•** meaning that bulkiness and polarity are antagonistic effects whose influences on *E* balance each other.

When $f(\varepsilon_r)$ is used as parameter, taking into account the errors, values are in the range 0.5 – 0.8, except for **6c•**. As expected, all values are positive. However, their influence is lower ($w_{f(\varepsilon r)}$ < 30%) than the influence of *c*. Indeed, $f(\varepsilon_r)$ describes only the effect of the polarity of the solvent, implying that the occurrence of H-bonding has a significant influence on the global solvent effect. However, KP relationships do not seem to be the best approach, as the polar effect of the solvent is either described by the polarity $f(\varepsilon_r)$ or by the Lewis acidity/electrophily *E*, and even in two cases (i.e., **1•** and **2•** in Table 9) by the polarizability.

To circumvent this issue, the KAT relationship (eq. (14)) was applied to **1•** - **7•**, affording good 3-parameter – π*, α, and *c* – correlations. The scattering of the plots E_T^N vs a_N (Figure 8 and Table 6) is significantly decreased, as highlighted by higher R^2 values, good *t*-test and *F*-test values (Table 11 and Figure 3SI). As given in eq. (16), E_T^N is a function of π* and α, and, as expected, KAT relationships are also based on π* and α but with different coefficients, e.g., for **5•**, $c_1 = c_3 = 0.33$, which are different from the coefficients given in eq. (16). Noteworthy, taking into account the errors, all nitroxides experience an effect of the same strength, due to the *structuredness* (cohesive pressure) of the solvent, although its influence (different w_c values) depends strikingly on the structure of the nitroxide, e.g., w_c = 12% for **1•** and **2•**, 20 – 23% for **3•** - **5•**, and 44 – 65% for **6•**/**7•**. Interestingly, for **1•** - **5•**, the HBD property is always the largest effect whereas, for **6•** and **7•**, HBD property α and polarity/polarizability π* are of the same size and clearly lower than the cohesive pressure *c*. Hence, *structuredness* is the major effect for **6•** and **7•**. Unfortunately, no rationale is available at this time.

The influence and the impact of the α, π* and *c* parameters for **1•** and **2•** have been previously discussed. Altough **3•** - **5•** exhibit very different polarities and bulkiness, the effect of the *structuredness* is the same. The same comment holds for π* and α effects.

In our case, the effect of parameters π* and α affords very similar results – i.e., the stabilization of the zwiterionic form **B** – and the discussion will only be provided for α. The highest HBD effects are reported for **1•** and **2•** (larger w_α). For **3•**, **4•**, and **5•**, the same HBD effect is observed whereas this effect is lower for **6•** and 7•. The HBD effect involves a hydrogen bond between the protic solvent and the nitroxyl moiety, and as a consequence, the stronger the interaction, the more favoured form **B**, the higher a_N.♪

The polarity/polarizability and hydrogen bonding effects strongly favour (positive sign for the coefficients) form **B** ($N^{+\bullet}$—O^- moiety), leading to an increase in a_N with increasing solvent properties. These effects are strengthened by the cohesive pressure *c* (positive sign for the coefficient) which is used to describe the *structuredness* of the solvent, i.e., a higher organization or a stronger solvent –solvent intereactions in the cybotactic region will strengthen the polarity/polarizability and H-bonding effects.

Multiparameter approach. Analysis of a_P.

As mentioned above, significant scattering was observed for the plots a_P against E_T^N for several nitroxides. The very popular KP and KAP relationships were applied to get deeper insight into the effects involved in the change in a_P. In contrast to the correlation with a_N, KAT and KP approaches are less general. Indeed, the KAT relationship (eq. (15)) is able to describe the solvent effect for **2•** - **7•** whereas KP relationship is only efficient for **5•** - **7•**.

Surprisingly, KP relationships cannot describe the solvent effect for **2•** - **4•**, whatever the combination of parameters. The solvent effect can be described by KP relationships using $f(\varepsilon_r)$ and *c*, however the correlations are significantly improved when the size of the solvent molecule V_M is included.

Interestingly, the coefficients of $f(\varepsilon_r)$, and *c* are negative, implying that $a_{\beta,P}$ values decrease with increasing properties. In fact, increasing $f(\varepsilon_r)$ and *c* leads to favour the zwiterionic forms of the N—O• (form **B**) and P=O (form **F**) moieties, and to favour the interaction between the $N^{+\bullet}$–O^-••••P^+–O^- moieties (form **H**) as described in Scheme 2, which, in turn, involved an increase in the dihedral angle θ affording a decrease in a_P.

On the other hand, the coefficient of the size of the solvent molecule V_M is positive, meaning that a_P increases with the size of the solvent molecule. That is, the bulkier the solvent is, the more hampered the PC—N bond rotation is, and the less favoured form **H** is. Taking into account the errors, the impact of V_M and ε_r is the same for all nitroxides and their influence is minor (w_{VM} < 27% and $w_{\varepsilon r}$ < 31%)) on the global solvent effect.

Unlike the KP relationship, KAT relationships are able to describe the solvent effect on a_P for all nitroxides, although this approach is marred by the number of outliers – 4 for **3•**, ca. 15 for **4•** and **5**. The steric effect for all nitroxides can be accounted for using π* and α as parameters. However, for **3•** and **4•**, the use of *c* as third parameter improves significantly the description of the data, although 14 outliers are still observed for **4•**.♫ Interestingly, the steric effect in **6•** and **7•** is well described using π* and *c* as parameters. The impact of α (w_α < 15%) is weak for **4•**, **6•** and **7•** whereas it is strong for **2•** and **5•**. The three effects have the same weight for **3•** in sharp contrast with other nitroxides. Except for **2•** and **5•**, the π* effect is the major effect. Unfortunately, there is no rationale at this time.

The negative slopes π* and *c* imply that a_P decreases with increasing properties. That is, the *structuredness* of the solvent in the cybotactic region affords better solvation of NO• and P=O moieties, leading to favour forms **B** and **F**, respectively,

through the π* effect of the solvent. Interestingly, for **2•**, **5•**, and **7•**, these comments hold for the α effect, *a contrario* of **3•**, **4•**, and **6•** which exhibit positive slopes. However, not too much importance will be given to these values, taking into account the low reliability of the coefficient d_3 for **6•** and to the large number of outliers for **3•** and **4•**. Nonetheless, these results are in good agreement with those observed for KP relationships, i.e., negative slopes for π*, $f(\varepsilon_r)$, and *c*.

It stems from comparing of KAT and KP relationships that the polarity (π* and $f(\varepsilon_r)$) and the size of the solvent molecules (V_X and V_M) are the main effects, which are antagonistic effects, ruling the change in a_P. The effect of α and of *c* is less obvious, as it does not apply to all nitroxides in the same series. Nevertheless, it seems strongly linked to the *stiffness* of the *structuredness* of the solvation cage around the nitroxyl moiety and maybe also around the phosphoryl group.

Although it has a negative coefficient, the polarity/polarizabity effect plays a role which is the same for a_P as for a_N, that is, increasing solvent polarity favours both form **B** and form **F**, implying stronger $N^{+\bullet}—O^{-}\cdots P^{+}—O^{-}$ interaction and, hence, a more stabilized form **H**. Amazingly, α and *c* do not apply to all nitroxides and can sometimes be interchanged, meaning that they do not describe their conventional effects. They both probably describe the organization of the solvent molecules around the N—O• and P=O moieties in the cybotactic region, meaning that the higher the *structuredness* (negative coefficients), the stronger the $N^{+\bullet}—O^{-}\cdots P^{+}—O^{-}$ interaction.

Conclusion

This survey of the solvent effect on new β-phosphorylated nitroxides **4•** - **7•** unveils an unexpected entanglement of effects, different for a_N and a_P, due to the various properties of the solvents. For all nitroxides, a_N is modified by the polarity/polarizability (π*), H-bonding (α), and *stiffness* of the *structuredness* (cohesive pressure *c*) of the solvents. On the other hand, the impact and the occurrence of each effect are less obvious for a_P than for a_N. The positive signs for π*, α, and *c* mean that a_N values increase with these solvent properties. On the other hand, the negative values for π*, α and *c* mean that a_P values decrease with these solvent properties. The anti-correlation between $a_{\beta,P}$ and a_N is ascribed to the $N^{+\bullet}—O^{-} \rightarrow P^{+}—O^{-}$ interaction whose maximization is the *driving force* of the system. This sensitivity of solvent might find interesting application in controlling the reduction/oxidation potential of nitroxide, which sensitive both to the bulkiness around the nitroxyl moiety and the polarity of the substituents.[34,35] The change in conformation might also use to investigate the presence of metal in solution as it might favoured the interaction with the nitroxyl moiety.[36]

Experimental section

^{1}H nuclear magnetic resonance (NMR) spectra were recorded using an internal deuterium lock at ambient temperatures on the following instruments: Bruker AC400 (400 MHz) and Bruker AC300 (300 MHz). Data are presented as follows: chemical shift (in ppm), integration, multiplicity (s = singlet, d = doublet, t = triplet, m = multiplet, br means the signal is broad, dd = doublet of doublets), coupling constant (*J* in Hz) and integration. ^{31}P NMR spectra were recorded on a Bruker AC300 (122 MHz) and on a Bruker AC400 (162 MHz) spectrometers with complete proton decoupling. Chemical shifts (δ) were reported in ppm using residual non-deuterated solvents as internal reference.[37]

High-resolution mass spectra (HRMS) were performed on a SYNAPT G2 HDMS (Waters) spectrometer equipped with atmospheric pression ionization source (API) pneumatically assisted. Samples were ionized by positive electrospray mode as follows: electrospray tension (ISV): 2800 V ; opening tension (OR): 20 V ; nebulization gas pression (nitrogen): 800 L/h. Low resolution mass spectra were recorded on ion trap AB SCIEX 3200 QTRAP equipped with an electrospray source. The parent ion (M^+, $[M+H]^+$, $[M+Na]^+$ or $[M+NH_4]^+$) is quoted.

Analytical thin layer chromatographies (TLC) were carried out on Merck Kieselgel 60 F254 plates. Flash column chromatographies were carried out on Merck Kieselgel 60 (230-400 mesh). Solvent system: gradients of DCM/MeOH; EtOAc/EtOH.

All experiments were performed under anhydrous conditions and an inert atmosphere of argon and, except where stated, using dried apparatus and employing standard techniques for handling air-sensitive materials. All reagents were weighed and handled in air at room temperature.

For EPR, samples were prepared at 0.5 mM nitroxide concentration in non-degassed solvents. Experiments were performed indifferently on Elexsys, EMX or ER 100D Bruker machines (a difference smaller than 0.1 G was noticed). EPR spectra were recorded, the parameters being a gain of 2 10^5 (72 dB for Elexsys), a modulation amplitude of 1.0 G, a sweep width of 150 G, a sweep time of 21 s, and a power of 20 mW.

All solvents and reactants were purchased from Aldrich and used as received. Nitroxides **3•**,[38] **4•**[39] and **6'•**,[40] and **7•**[22] were prepared according to the literature. Nitroxides **5'•, 5•** and **6•**, were prepared according to Scheme 1.

Diethyl (1-((1-hydroxy-2-methylpropan-2-yl)amino)-2-methylpropyl)phosphonate (5).

Isobutyraldehyde (5 g, 69 mmol) and 2-amino-2-methylpropan-1-ol (6.2 g, 69 mmol) were mixed and stirred at room temperature for 24 h. Molecular sieves (4Å, n g) were added, followed by diethylphosphite (14.4 g, 104 mmol). After stirring the resulting mixture for 7 d, it was diluted with dichloromethane and acidified with aq. HCl solution. The aqueous phase was then washed with dichloromethane, then solid $NaHCO_3$ was added until pH was basic. After extraction with dichloromethane, the organic phase was dried and concentrated *in vacuo* to give **5** (14.0 g, 50 mmol, 72%) as a colorless oil. ^{1}H NMR ($CDCl_3$, 400 MHz): δ = 4.66 (br s, 1H), 4.22-4.04 (m, 4H), 3.41 (d, *J* = 11.8 Hz, 1H), 3.09 (d, *J* = 11.8 Hz), 2.88 (dd, *J* = 17.7, 3.3 Hz, 1H), 1.96 (ddhept, *J* = 18.8, 7.0, 3.3 Hz, 1H), 1.32 (t, *J* = 6.8 Hz, 3H), 1.31 (t, *J* = 7.1 Hz, 3H), 1.09

(s, 3H), 1.01 (d, *J* = 7.0 Hz, 3H), 0.96 (d, *J* = 7.0 Hz, 3H), 0.93 (s, 3H); ^{13}C NMR ($CDCl_3$, 75 MHz): δ = 68.4, 62.7 (d, *J* = 8.0 Hz), 61.6 (d, *J* = 7.9 Hz), 54.3 (d, *J* = 4.7 Hz), 54.1 (d, *J* = 147.1 Hz), 31.1 (d, *J* = 5.5 Hz), 26.6, 23.3, 19.9 (d, *J* = 11.5 Hz), 18.3 (d, *J* = 2.1 Hz), 16.4 (d, *J* = 5.5 Hz), 16.3 (d, *J* = 5.7 Hz); ^{31}P NMR ($CDCl_3$, 162 MHz): δ = 31.1; HRMS: Calcd for $C_{12}H_{29}NO_4P^+$ $[M+H]^+$ 282.1829, Found 282.1828.

4-(diethoxyphosphoryl)-1-hydroxy-2,2,5-trimethyl-3-azahexan-3-oxyl radic al 5'•.

To a stirred solution of aminophosphonate **5** (100 mg, 0.36 mmol) in dichloromethane (5 mL) was added *meta*-chloroperbenzoic acid (70% in water, 131 mg, 0.53 mmol). After stirring the mixture for 24 h, it was diluted with dichloromethane, washed with aq. sat. $NaHCO_3$ solution, dried and concentrated *in vacuo*. Colum chromatography of the residue gave **5'•** (61 mg, 0.21 mmol, 58 %) as an orange oil. HRMS: Calcd for $C_{12}H_{28}NO_5PNa^+$ $[M+Na]^+$ 319.1519, Found 319.1517.

1-acetoxy-4-(diethoxyphosphoryl)-2,2,5-trimethyl-3-azahexan-3-oxyl radical 5•.

To a stirred solution of nitroxide **5'•** (50 mg, 0.17 mmol) in dichloromethane/pyridine mixture (1:1, 4 mL) was added acetic anhydride (26 mg, 0.25 mmol). After stirring the mixture for 24 h, it was diluted with dichloromethane, washed with aq. HCl solution, washed with aq. sat. $NaHCO_3$ solution, dried and concentrated *in vacuo*. Colum chromatography of the residue gave **5•** (52 mg, 0.15 mmol, 91 %) as an orange oil. HRMS: Calcd for $C_{14}H_{30}NO_6P^+$ $[M+H]^+$ 339.1805, Found 339.1807.

1-acetoxy-4-(diethoxyphosphoryl)-2,2,5,5-tetramethyl-3-azahexan-3-oxyl radical 6•

To a solution of alcohol **6'•** (300 mg, 0.97 mmol) in DCM (10 mL) at room temperature under argon was added Et_3N (293 mg, 2.90 mmol), a catalytic amount of DMAP and acetic anhydride (148 mg, 1.45 mmol). The mixture was stirred for 8 hours. Then, the mixture was poured on a saturated solution of $NaHCO_3$ and extracted with DCM. The organic layer was dried with $MgSO_4$ and the solvent removed *in vacuo*. The crude product was purified by flash chromatography to afford product **6•**, 247 mg, yield 72%. HRMS (ESI) calc for $C_{15}H_{32}NO_6P^+$•: 353.1962 $[M+H]^+$; found: 353.1962.

Acknowledgements

The authors thank Aix-Marseille University and CNRS for financial support. ANR was granted for funding this project (grants SonRadIs ANR-11-JS07-002-01 and NITROMRI ANR-09-BLA-0017-01). LB is thankful to ANR for the Ph.D. fellowship (grant SonRadIs). SRAM thanks the Russian Science Foundation (grant 15-13-20020) for supporting the correlation analysis of this work. The authors thank RENARD network for the EPR platform.

Notes and references

As far as we know, this nitroxide has only been observed through spin-trapping experiments involving the addition of 2-diethoxyphoshorylprop-2-yl radical onto *tert*-butyl nitroso. Consequently, its preparation on a large scale by conventional procedures is not so obvious.

§ θ the dihedral angle between the C—P bond and the Singly Occupied Molecular Orbital SOMO (Figure 2) on the nitrogen atom of the nitroxyl moiety. ρ_N^{π}, the electron density on the nitrogen atom of the nitroxyl moiety, is proportional to the a_N value. B_0¥ is the transfer of the spin density through the spin polarization process and B_1‡ is the transfer of the spin density through the hyperconjugation process.

¥ In general, B_0 is very small and can be neglected. See ref. 9.

‡ Values of B_1 are dependent on the atom or on the function at position β. See refs. 19 and 9.

† As all figures were very similar.

Ω Janzen and coll. in ref. 17 reported the same solvent effect (only benzene, methanol, and water were investigated) for some β-phosphorylated nitroxides. They tentatively ascribed this effect to a change in conformation due to a difference in polarity of the mesomeric forms. Nevertheless, their discussion is very ambiguous and their schemes not convincing, although they might agree with our proposal.

√ Many other parameters available in the literature can be used to describe the different terms of eq. 22. Here, only the parameters used for the KP and KAT correlations are discussed.

♪ For the π* effect, the polarity/polarizability of the solvent will stabilize form **B**.

♫ Parameter α is not significant for a two-parameter KAT relationship.

1 G. Likhtenshtein, J. Yamauchi, S. Nakatsuji, A. I. Smirnov, R.Tamura, Nitroxides: Applications in Chemistry, Biomedicine, and Materials Science, Wiley-VCH, 2008, and references therein.
2 Stable Radicals: Fundamentals and Applied Aspects of Odd-Electron Compounds (Ed.: R. Hicks), Wiley, Hoboken, 2010, pp. 173–229, and references therein.
3 I. A. Kirilyuk, A. A. Bobko, V. V. Khramtsov, I. A. Grigor'ev, *Org. Biomol. Chem.*, 2005, **3**, 1269–1274.
4 V. Belle, S. Rouger, S. Costanzo, A. Longhi, A. Fournel, Assessing Structures and Conformations of Intrinsically Disordered Proteins (Ed.: V.N. Uversky), Wiley, Hoboken, 2009, and references cited therein.
5 P. Mellet, P. Massot, G. Madelin, S. R. A. Marque, E. Harte, J.-M. Franconi, E. Thiaudière, *PLoS One*, 2009, **4**, e5244.
6 H. Karoui, F. Le Moigne, O. Ouari, P. Tordo, *Stable Radicals: Fundamentals and Applied Aspects of Odd-Electron*

Compounds, ed. R. Hicks, John Wiley & Sons, 2010, pp. 173–229.
7 V. Ovcharenko, *Stable Radicals: Fundamentals and Applied Aspects of Odd-Electron Compounds*, ed. R. Hicks, John Wiley & Sons, 2010, pp. 461–506.
8 B. Knauer, J. J. Napier, *J. Am. Chem. Soc.,* 1976, **98**, 4395 – 4400.
9 E. G. Janzen, G. A. Coulter, U. M. Oehler, J. P. Bergsma, *Can. J. Chem.*, 1982, **60**, 2725–2733.
10 C.-H. Deng, C.-J. Guan, M.-H. Shen, C.-X. Zhao, *J. Fluorine Chem.*, 2002, **116**, 109–115.
11 A. Sh. Mukhtarov, A. V. Il'Yasov, Ya. A. Levin, I. P. Gozman, M. S. Skorobogatova, E. I. Zoroatskaya, *Theor. Exp. Chem.* **1976**, *12*, 656–660; *Teor. Eksp. Khim.,* 1976, **12**, 831 – 836.
12 C. Reichardt, T. Welton, Solvent and Solvent Effect in Organic Chemistry, 4th ed., Wiley-VCH, Weinheim, **2011**.
13 S. Marque, C. Le Mercier, P. Tordo, H. Fischer, *Macromolecules*, 2000, **33**, 12, 4403-4410.
14 G. Audran, P. Brémond, S. R. A. Marque, G. Obame, *ChemPhysChem* 2012, **13**, 15, 3542-3548.
15 G. Audran, L. Bosco, P. Brémond, T. Butscher, S. R. A. Marque, *Appl. Magn. Reson.* 2015, **45**, 12, 1333-1342.
16 G. Audran, L. Bosco, P. Brémond, T. Butscher, S. R. A. Marque *Org. Biomol. Chem.* 2016, **14**, 1228-1292.
17 . D. L. Haire, E. G. Janzen, G. Chen, V. J. Robinson, I. Hrvoic, *Magn. Reson. Chem.,* 1999, **37**, 251-258.
18 G. Audran, L. Bosco, P. Brémond, T. Butscher, J.-M. Franconi, K. Kabitaev, S. R. A. Marque, P. Mellet, E. Parzy, M. Santelli, E. Thiaudière, S. Viel *RSC Advances* 2016, **6**, 5653-5670.
19 F. Gerson, W. Huber, Electron Spin Resonance Spectroscopy of Organic Radicals, Wiley-VCH, Weinheim, 2003.
20 Nitroxide Mediated Polymerization: From Fundamentals to Applications in Materials Science Series: RSC Polymer Chemistry Series Ed. D. Gigmes, 2015.
21 J. Nicolas, Y. Guillaneuf, C. Lefay, D. Bertin, D. Gigmes, B. Charleux Prog. Polym. Sci. 2013, **38**, 63-235.
22 G. Audran, L. Bosco, P. Brémond, T. Butscher, J.-M. Franconi, S. R. A. Marque, P. Mellet, E. Parzy, M. Santelli, E. Thiaudière *Org. Biomol. Chem.* 2015*,* **13**, 11393-11400.
23 [23] S. Marque *J. Org. Chem.* 2003, **68**, 20, 7582-7590.
24 M. Charton, *Prog. Phys. Org. Chem.*, 1981, **13**, 119-251.
25 E. G. Bagryanskaya, S. R. A. Marque, *Chem. Rev.* 2014, **114**, 5011-5056.
26 T. Fujita, C. Takayama, M. Nakajima, *J. Org. Chem.* 1973, **38**, 1623–1630.
27 Y. Marcus, *The Properties of Solvents*, Vol. 4, Wiley, Chichester, 1998.
28 G. E. Zaikov, R. G. Makitra, G. G. Midyana, L. I. Bazylyak, *Influence of the Solvent on Some Radical Reaction* Chemistry Research and Applications Series, Nova Science Publishers Inc., New York, 2010.
29 J. Shorter, Correlation Analysis of Organic Reactivity; J. Wiley & Sons: New York, 1982, 73-126.
30 J. Shorter, Correlation Analysis of Organic Reactivity; J. Wiley & Sons: New York, 1982, 9-25.
31 E. G. Bagryanskaya, S. R. A. Marque, Y. P. Tsentalovich *J. Org. Chem.* 2012, **77**, 11, 4996-5005.
32 A. R. Katritzky, D. C. Fara, H. F. Yang, K. Tamm, T. Tamm, M. Karelson, *Chem. Rev.*, 2004, **104**, 175-198.
33 I. A. Koppel, V. A. Palm, The Influence of the Solvent on Organic Reactivity, in N. B. Chapman and J. Shorter (Eds.): Advances in Linear Free Energy Relationships, Plenum Press, London, New York, 1972, Chapter 5, p. 203.
34 I. A. Kirilyuk, A. A. Bobko, S. V. Semenov, D. A. Komarov, I. G. Irtegova, I. A. Grigor'ev, E. Bagryanskaya, *J. Org. Chem.* 2015, **80**, 91-18-91-25.
35 E. Zottler, G. Geischeidt, *J. Chem. Res.* 2011, 257-267.
36 E. G. Kovaleva, L. S. Molochnikov, V. A. Osipova, D. P. Stepanova, V. A. Reznikov, *Appl. Magn. Reson.* 2015, **46**, 1367-1382.
37 H. E. Gottlieb, V. Kotlyar, A. Nudelman, *J. Org. Chem*. 1997, **62**, 7512.
38 D. Benoit, V. Chaplinski, R. Braslau, C. J. Hawker, *J. Am. Chem. Soc.* 1999, **121**, 3904–3920.
39 A. Acerbis, E. Beaudoin, D. Bertin, D. Gigmes, S. Marque, P. Tordo, *Macromol. Chem. Phys.* 2004, **205**, 7, 973-978
40 S. Acerbis, D. Bertin, B. Boutevin, D. Gigmes, P. Lacroix-Desmazes, C. Le Mercier, J.-F. Lutz, S. R. A. Marque, D. Siri, P. Tordo *Helv. Chim. Acta* 2006, **89**, 10, 2119-2132.